2014

# An Experimental Study of the C-Start of a Mechanical Fish

Benjamin Kandaswamy Chinna Thambi
*University of Massachusetts - Amherst*, bkandasw@umass.edu

# AN EXPERIMENTAL STUDY OF THE C-START OF A MECHANICAL FISH

A Thesis Presented

by

BENJAMIN KANDASWAMY CHINNA THAMBI

Submitted to the Graduate School of the
University of Massachusetts Amherst in partial fulfillment
of the requirements for the degree of

MASTER OF SCIENCE IN MECHANICAL ENGINEERING

SEPTEMBER 2014

Department of Mechanical and Industrial Engineering

**AN EXPERIMENTAL STUDY OF THE C-START OF A MECHANICAL FISH**

A Thesis Presented

by

BENJAMIN KANDASWAMY CHINNA THAMBI

Approved as to style and content by:

_____
Yahya Modarres-Sadeghi, Chair

_____
Sundar Krishnamurty, Member

_____
Yossi Chait, Member

_____
Donald L. Fisher, Professor and Department Head,
Department of Mechanical & Industrial Engineering

**ACKNOWLEDGEMENTS**

I would like to thank my advisor, Professor Yahya Modarres-Sadeghi, for his able guidance and support throughout the course of this project. I also thank Professor Sundar Krishnamurty and Professor Yossi Chait for agreeing to serve on the committee for this thesis and for their support and advice when I needed.

I also thank all my lab mates and friends who were always willing to help.

**ABSTRACT**

AN EXPERIMENTAL STUDY OF THE C-START OF A MECHANICAL FISH

SEPTEMBER 2014

BENJAMIN KANDASWAMY CHINNA THAMBI, B.S.M.E, SWAMY VIVEKANANDA INSTITUTE OF TECHNOLOGY

M.S.M.E, UNIVERSITY OF MASSACHUSETTS AMHERST

Directed by: Professor Yahya Modarres-Sadeghi

The Northern Pike have recorded the highest accelerations for marine propulsors. The mean peak acceleration and velocity for a number of trials were found to be 120 $ms^{-2}$ and 4 $ms^{-1}$ respectively (Harper and Blake 1990) for live fish. Here, we emulate this fast-start motion and analyze the performance of the Northern Pike, using a mechanical fish.

The mechanical fish was made of a PVC head attached to a spring steel frame with aluminum ribs and a plastic tail. A latex rubber sheet was used as the skin of the fish. The set-up used air bearings for frictionless motion with two degrees of freedom. The fish was bent to a C shape using servo motors. The two stages of the fast-start motion of a live fish with preparatory and propulsive strokes were closely replicated with this experimental set-up. The results showed that the acceleration profiles were qualitatively similar to that of the live fish.

The objective of this project was to understand the mechanism by which the high acceleration is achieved in live fish. The designed mechanical fish was used to quantify the influence of the timing of each stroke and the shape and stiffness of the tail on the observed peak acceleration.

**TABLE OF CONTENTS**

Page

**LIST OF TABLES**

Table Page

**LIST OF FIGURES**

# CHAPTER 1

# INTRODUCTION

The Locomotion of marine animals has been the source of inspiration for many manmade vehicles for a long time. The acceleration achieved by some marine mammals far exceeds the acceleration achieved by any manmade vehicle. The fast-start fishes have recorded some very high accelerations. The fish with the highest recorded fast-start acceleration is the northern pike. If manmade underwater vehicles could replicate even a fraction of this hydrodynamic performance, it would greatly increase their efficiency and maneuverability, resulting in higher speeds and smaller turning radius.

The objective of this study is to investigate the factors responsible for the high acceleration observed in the pike by emulating the fast-start motion of the live fish using a mechanical fish. A series of experiments will be conducted using a mechanical fish and the forward acceleration of the fish will be measured when parameters such as the size and shape of the fish tail, body stiffness, body curvature, and stroke timing will vary. The goal here is not to try and achieve the high accelerations observed in the live fish, but rather compare the relative hydrodynamic performance of the mechanical fish to that of the live fish with varying parameters.

## 1.1 Northern Pike (Esox Lucius)

The Northern pike fish is termed as a fast-start specialist and has peak accelerations higher than those recorded for a generalist fish like trout. Harper and Blake (1990) conducted a series of experiments on live pike fish to study their fast-start response. They measured the response of the pike during Escape Response (ER) and Feeding Strike (FS) motions using subcutaneously placed accelerometers in the fish. They found the mean peak acceleration to be 150 $ms^{-2}$ for Escape Response and 120 $ms^{-2}$ for Feeding Strike, with one trial recording an

acceleration of 250 $ms^{-2}$. These high accelerations are possible because of the high muscle power to mass ratio. Fishes generally have two types of muscle: Red muscles which have more stamina but contract at a slower rate and white muscles which have less stamina but contract much faster which is suitable for quick bursts of energy characteristic of fast starts.

**1.2 Fish Locomotion**

Fish locomotion has been of interest to biologists and engineers alike and hence is one of the focal points of investigation in the blooming field of biomimetics research. The anatomy of a fish is shown in Figure 1. Fishes have known to be very efficient swimmers and adapt to conditions very well. The fish uses its body to push the fluid around it and the momentum it imparts to the fluid provides the reaction force or thrust to propel the fish forward. It then either uses its head or its fins to change direction. The lift force has to be greater than its weight and the thrust generated must be greater than the drag force for the fish to move forward. The undulatory motion of fishes, employed for swimming, enables them to reduce drag and also to minimize turbulence in the wake (Barrett 1999). The undulatory propulsion of fish has been the

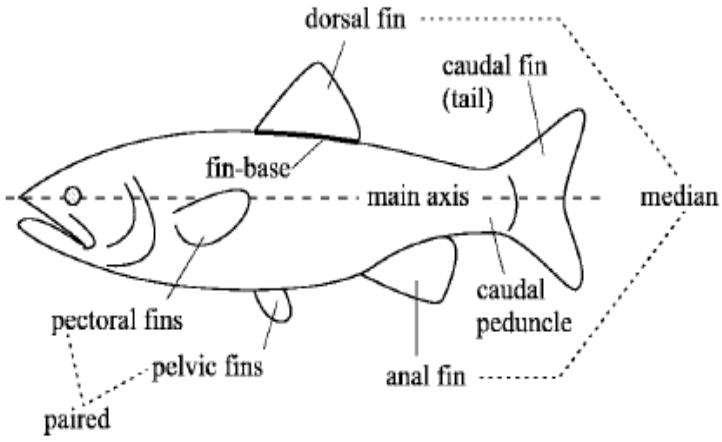


**Figure 1. Anatomy of a Fish (Figure from Sfakiotakis et al. 1999)**

subject of investigation following the classic studies of Gray (1936) when he argued that the theoretical drag on dolphins was several times greater than the drag observed for a similar rigid models and the drag exceeded the maximum muscle power of the dolphin.

**1.3 Swimming Modes**

Fish swimming has been generally classified into modes based on the species (Breder, 1926; Lindsey, 1978). When large portions of the fish body undergo undulatory motion, they are called as Anguilliform swimmers. Anguilliform swimmers like eels have an undulatory motion which uses their entire body to send a travelling wave from head to tail to achieve propulsion. Carangiform swimmers like sharks use only the posterior portion of their body to achieve propulsion. This mode of locomotion is termed as Body Caudal Fin locomotion (BCF) (Webb 1984). Thunniform swimmers employ only their caudal fin for propulsion and are known to swim long distances while some other fishes use Median Paired Fins (MPF) (Webb 1984) to navigate in the water (Figure 2). Of particular interest to us is the BCF mode of propulsion which is used for high speed swimming. Swimming in fishes can be further classified as steady swimming or periodic swimming, which is seen in long distance swimmers like tuna, and unsteady swimming or transient mode of propulsion, in which the fish uses large unsteady forces to achieve very high accelerations. The latter mode of propulsion is generally called as a fast-start motion.

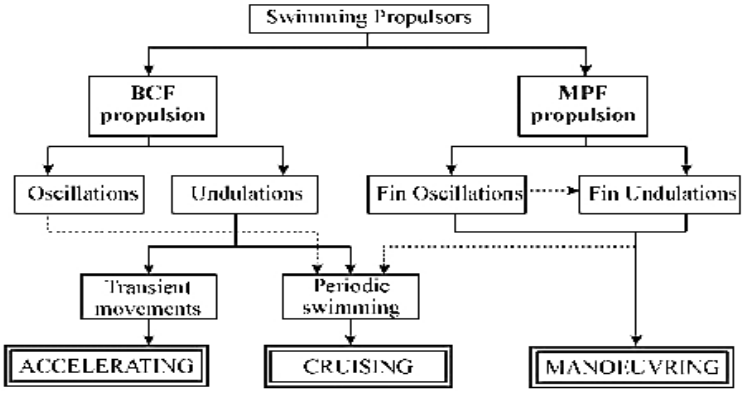


**Figure 2. Different swimming modes (From Sfakiotakis et al. 1999)**

### 1.3.1 Fast-Start Motion

Fast starts are high-energy swimming bursts starting from the rest or imposed upon periods of steady swimming (Domenici & Blake 1997). Weihs described the fast-start maneuver in three stages. Namely, the Preparatory stage in which the fish bends its body to either a C or an S-shape which is followed by the Propulsive stage, which involves an aggressive uncoiling of the fish which sends a travelling wave along the body of the fish to propel it forward. The third stage can comprise of subsequent propulsive strokes or simply coasting. There are two types of fast-start motions that are observed in fish: the C-shape fast-start and the S-shape fast-start.

#### 1.3.1.1 C-Shaped Fast-Start

C-shape fast-starts involve the fish bending to a C-shape during the preparatory stage. The C starts are used by fish to escape from prey during predator-prey interactions. It is typically termed as an Escape Response (ER). The C-starts have a large turning angle and a sharp angle of attack of the caudal fin, which results in higher accelerations compared to the S-start. The C-start also has a significant change in the direction of the fish after the motion is completed. This is done so that the fish can escape its predator by rapidly changing direction and also to have a small turning radius which is smaller than the turning radius of its predator. Biologists have shown that the C-start is achieved by contracting all the muscles on one side of the fish by means of the Mauthner neurons in the fish. The Mauthner cells are a pair of reticulospinal neurons with axons which extend to the entire spinal cord (Tytell and Lauder, 2006). The M-cells were found to be crucial in the escape response of gold fish (Zottoli, 1977; Eaton et al., 1981) and are the fastest conducting fibers in the nervous system of the fish (Funch et al., 1981). The modulation of the sensory information by the M-cells results in large-amplitude body bending in the fish.

#### 1.3.1.2 S-Shaped Fast Start

The S-starts involve the fish bending to an S shape during the preparatory stage. The S-starts are used by the fish to hunt prey and are hence termed as Feeding Strikes (FS). The S-starts do not involve a change in direction of the fish and the fish head is coincident with the axis of the midline of the fish after the propulsion stage. This makes sense as the fish has to orient itself in a straight line path which intersects with its prey so that it can intercept it. Not much is known about the method of neuron firing for the S-starts. The S-starts have lower peak accelerations. There are several studies on the fast-start of the live fish. Table 1 gives a summary of the results based on those studies.

**Table 1. Summary of some of the studies done on Fast-starts in fish (From Domenici and Blake, 1997)**

| Authors | Common Name | Fast-Start Type | Method (Hz) | Maximum Acceleration ($ms^{-2}$) | Maximum Velocity ($Ls^{-1}$,$ms^{-1}$) | Duration (ms) | Body Length (m) |
|---|---|---|---|---|---|---|---|
| Weihs (1973) | Pike | ER | 40 | 50 | - | - | - |
| Webb (1978) | Tiger musky | ER | 250 | 39.5 | 7.2, 1.6 | 115 | 0.217 |
| Rand and Lauder (1981) | Chain pickerel | FS | 200 | 21.1 (mean) | 9.0, 2.5 | 92 | 0.273 |
| Webb (1986) | Tiger musky | ER | 60 | 15 (mean) | 21, 1.4 | - | 0.065 |
| Harper and Blake (1991) | Northern pike | ER | Acc | 120.2 (mean) | 10.5, 3.97 | 108 | 0.378 |
| Harper and Blake (1991) | Northern pike | FS | Acc | 95.9 (mean) | 8.2, 3.1 | 133 | 0.378 |
| Frith and Blake (1991) | Northern pike | ER | 250 | 151.3 (mean) | 8.7, 3.5 | 129 | 0.400 |

### 1.4 Mechanical Pike

To be able to study the fast-start motion of fish, mechanical models have been built and tested yielding good results (Trianatafyllou et al. 1995; Conte et al. 2010). Conte et al. designed and built a simple mechanical fish modeled after the Northern Pike because of its superior performance characteristics of fast start motion. Their mechanical fish achieved a peak acceleration of 40 $ms^{-2}$. The fish comprised of a thin metal beam covered with polyurethane rubber and attached with an appropriately shaped tail (Figure 3). The fish was held in a bent C shape by two restraining lines which were simultaneously released to propel the fish forward.

**Figure 3. The Mechanical Pike fish designed by Conte et al. 2010.**

Although the peak acceleration they observed was smaller than the live fish, the form of the acceleration time history was very similar to that of the live fish, as measured by Harper and Blake (1990) (Figure 4).

The angle of bending of the fish to achieve the optimal kinetic energy upon release was calculated to be 90 degrees. The efficiency of the mechanical fish was found to be around 10%, compared to the range of efficiencies calculated for live fish which are 16%-39% (Frith and Blake 1995).

This simple mechanical system emulated the base forms of time varying acceleration, velocity and displacement of the live fish closely even though it did not have the preparatory stroke and was a single stage propulsion. It also did not have the travelling wave along the fish body, which is observed in live fish. Ahlborn (1997) emphasized the importance of the interaction between the vortices shed by the tail tip during the preparatory stroke with the vortices shed during the propulsive stroke. It was postulated that the momentum transfer takes place between the two counter rotating vortices. Thus, the presence of the preparatory stroke will enable the mechanical fish to emulate the behavior of the live fish even more closely. These features were taken into consideration toward designing a second mechanical fish as will be discussed in Chapter 2. The results from the tests investigating the performance of this fish with varying parameters of tail stiffness, tail size and bending curvature will be discussed along with the future work in the subsequent chapters.

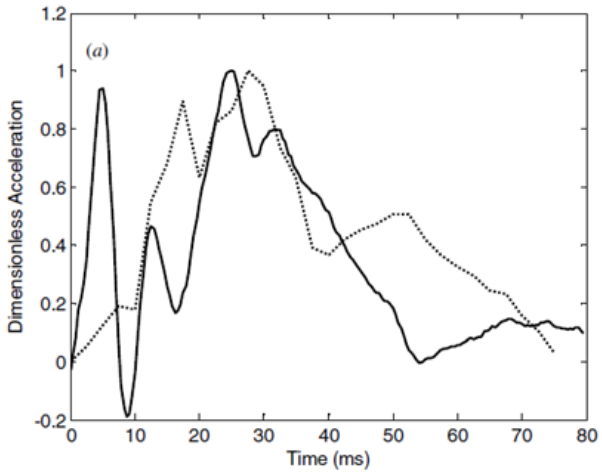


**Figure 4. The dimensionless acceleration of the mechanical pike compared to that of the live fish as measured by Harper and Blake (1990) shown by the dotted line. (Figure from Conte et al. 2010)**

## CHAPTER 2

## THE EXPERIMENTAL SET-UP

### 2.1 The Mechanical Fish

The new mechanical fish is capable of performing the preparatory stroke as well as the propulsive stroke (Feng et al. 2011). The previous version of the fish was passively propelled as it consisted of only the propulsive stage (Conte et al. 2010). The new mechanical fish allows varying different parameters such as the body stiffness, duration of the preparatory and propulsive stages, the speed of bending and the bending curvature.

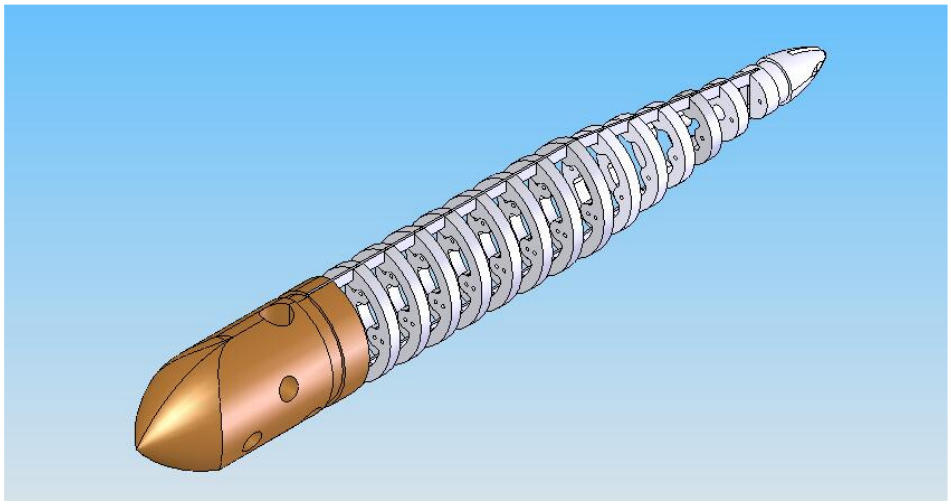

**Figure 5. 3D model of the second generation mechanical pike**

The fish body has a spring steel frame which acts as the spine of the fish. Aluminum ribs are attached along the length of the spine. The spine is attached to a PVC head. The fish body is designed to have a similar cross-sectional area to that of the live pike (Figure 5). The advantage of the second generation mechanical fish is that it can be assembled in different configurations by varying individual components like the head, tail and spine. The previous version of the fish was limited in its scope for varying these parameters. The current mechanical fish bent to a C-shape is shown in Figure 6.

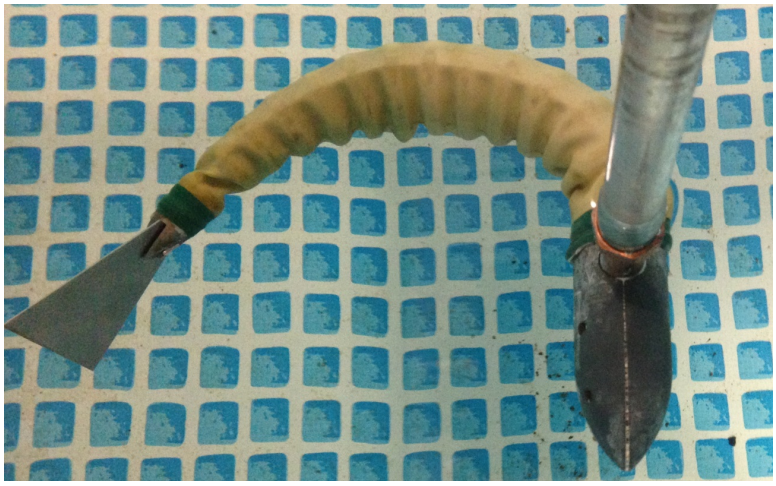

**Figure 6. Mechanical fish bent to a C-shape**

### 2.1.1 Test Rig

The test rig was a rectangular frame with four legs, built with extruded aluminum. The rig supports the guide surfaces which allowed the fish to move in the forward and transverse directions. A drawing of the test rig is shown in Figure 7.

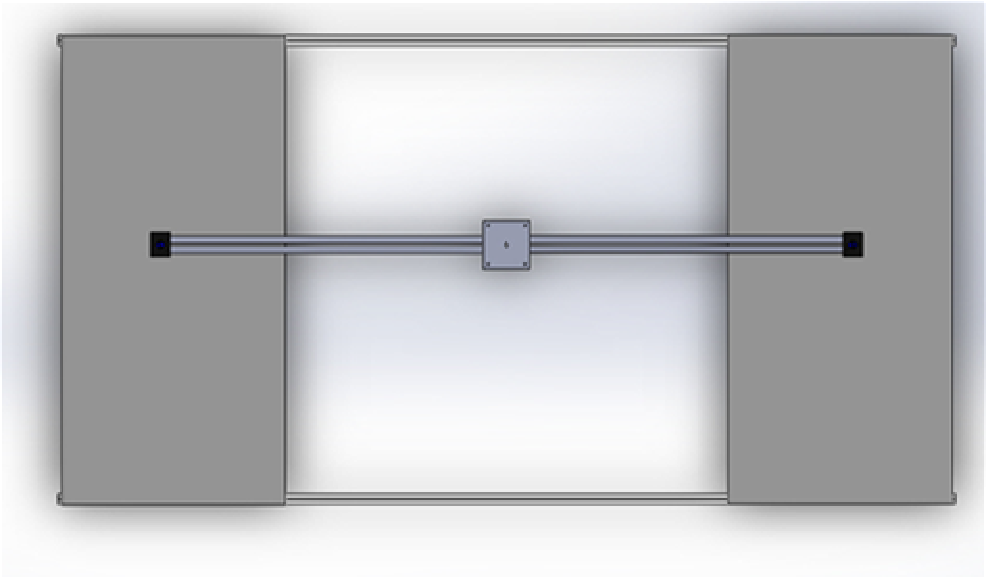

**Figure 7. Top-view of the Test rig which supports the fish set-up**

The fish was suspended from a platform by means of a stainless steel rod. The platform was connected to aluminum rods fitted with end blocks which were mounted on air-bearings to allow frictionless motion of the fish. The air bearings glide along the guide surfaces which are supported by the test rig. Glass sheets were used as the guide surfaces for the air-bearings. The test setup with the fish is shown in Figure 8. The test section was a metal frame pool with dimensions of 96”x59”x24” which allowed for ample distance from the fish to the side walls of the test section.

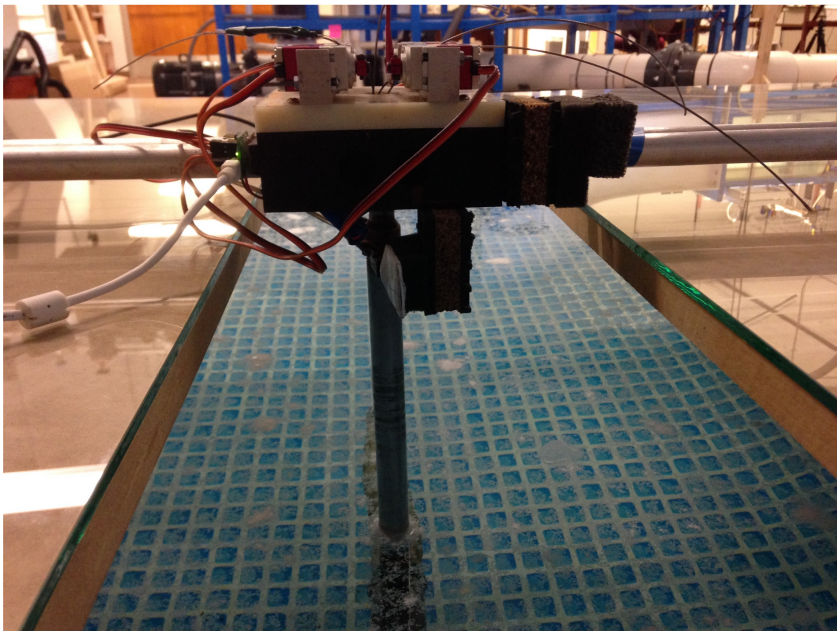

**Figure 8. The Mechanical fish set-up**

### 2.2.2 Actuators

High-torque servo motors were used to bend and unbend the fish. The servo motors were mounted on a block from which the fish was suspended. The servos used were JR high speed RC airplane servos which had a stainless steel housing and a torque of 480 oz-in with a speed of rotation of 60 degrees in 0.15 seconds. The servos had a relatively high power-to-weight ratio which worked well for this experiment.

### 2.2.3 Interface

The servo motors were controlled by a USB-6 channel servo controller which was powered by a 5V DC power supply. The Microcontroller used in this setup is shown in Figure 9.

**Figure 9. Pololu 6-Channel USB servo controller**

The servo controller was connected to a computer which was then able to control the speed and timing of the servos with simple scripts.

### 2.2.4 Measuring devices

A 3-axis accelerometer, mounted on the platform above the fish head and aligned to the center of its axis, was used to measure the acceleration. The accelerometer had a sampling frequency of 1000 Hz and measured acceleration of up to 2g with an acceptable precision. The accelerometer is shown in Figure 10.

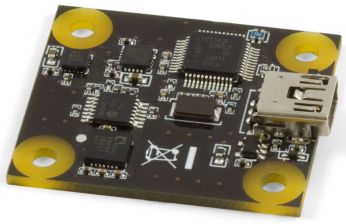

**Figure 10. Phidgets 1043 3-axis accelerometer**

The Accelerometer was connected via a USB to a computer where the measured acceleration was recorded. To calculate the duration of the preparatory and propulsive strokes and also measure the angle of bending of the fish, a Lumix camera which records at 240 frames per second at a resolution of 640 X 480 was used. The diagram illustrating the interconnections of the measuring devices, actuators and interfaces with the setup is shown in Figure 11.

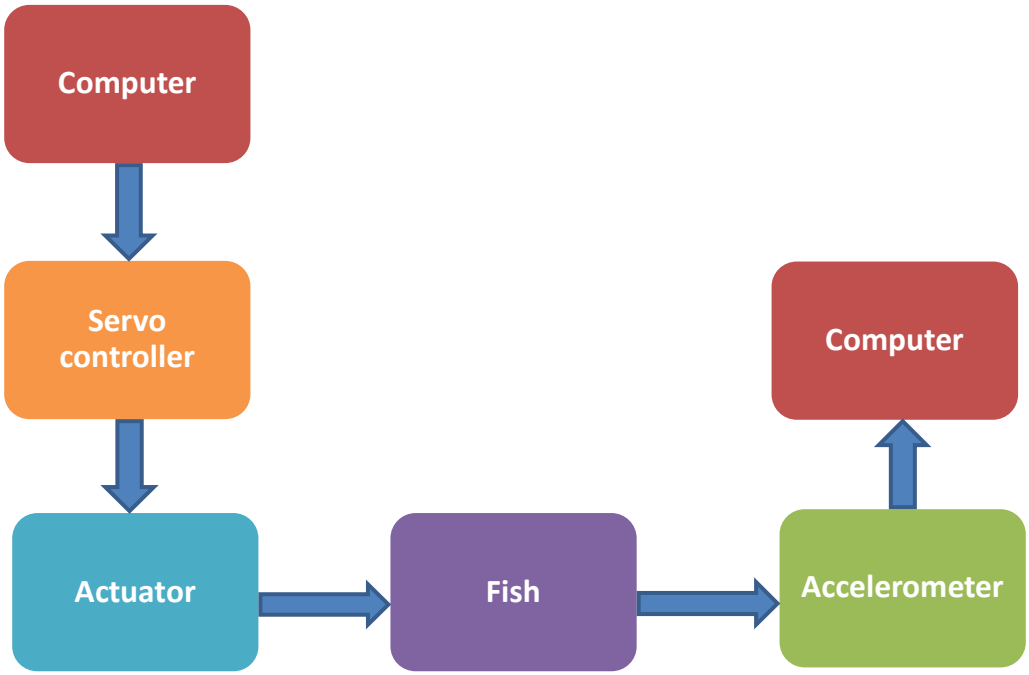


**Figure 11. Flow chart of the fish set up**

### 2.2.5 Working Mechanism

Stainless steel brake cables were threaded along the body of the fish which when pulled, bent the fish in the corresponding direction and unbent it upon releasing. The cable made a sharp bend near the fish head to attach to the servos overhead and thus brake-cable housing was used to reduce the friction of the moving wires and ensure a smooth motion. The working mechanism is illustrated in Figure 12.

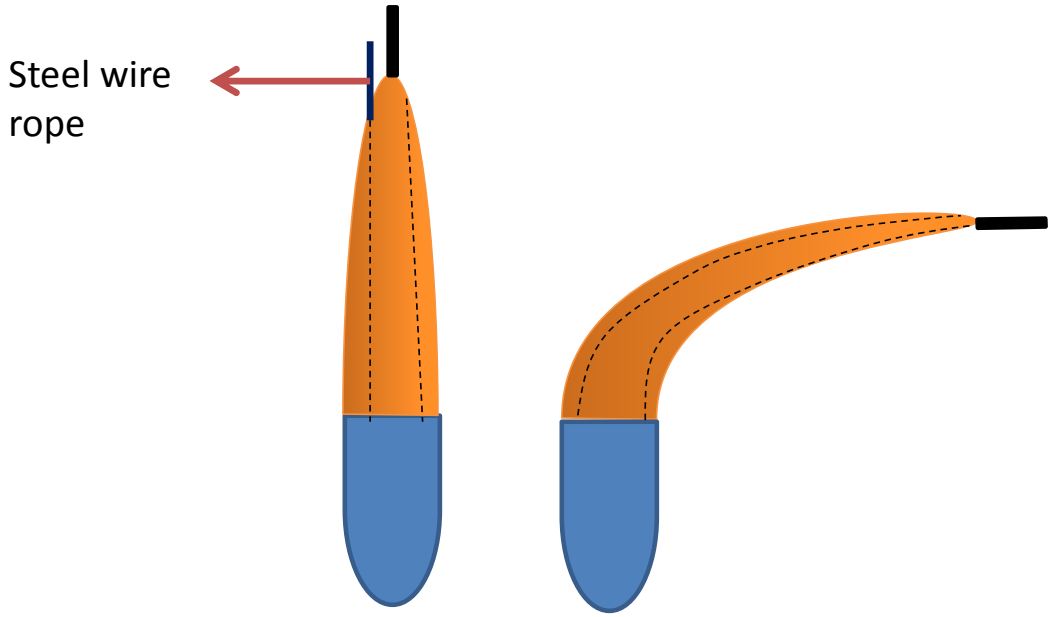


**Figure 12. Diagram showing the working mechanism of the fish**

From the figure we can see that the fish bends in a direction toward the side of the cable which is pulling it. Sufficient slack should be allowed on the other side as seen in the figure, to allow the fish to bend. In the current experiments, the fish was forcibly unbent by pulling on the opposite cable, when the servo bending the fish to one side released it. This forced unbending increased the speed of the propulsive stroke.

**2.2.6 Filtering the signal**

Since the Accelerometer was mounted on a platform housing moving, there were vibrations inherent in the system which could not be avoided. In order to identify the frequency range of the noise and filter it out, the accelerometer reading when the servos were switched on was recorded and a Fast Fourier Transform was performed on the signal as shown in Figure 13. A distinct peak was observed at 300 Hz. A Notch Filter was thus used to remove this noise in the system.

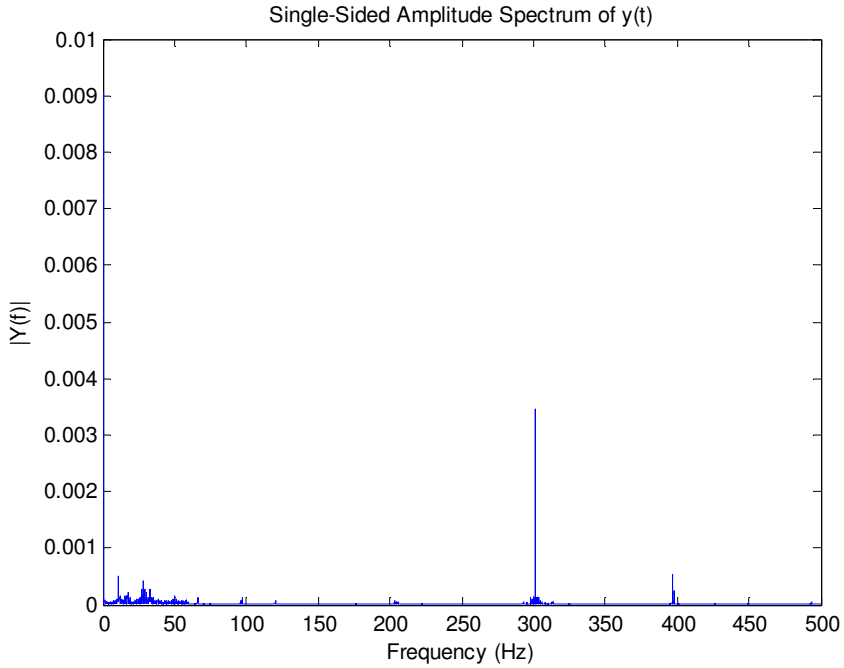


**Figure 13. Fast Fourier Transform of the servo vibration**

Besides filtering the signal, additional measures were taken to reduce the effect of system vibrations by placing the accelerometer on an anti-vibration mount and a sponge. The anti vibration mount was a block of cork wood sandwiched with neoprene rubber as shown in Figure 14.

**Figure 14. Anti-vibration mount for the accelerometer**

## CHAPTER 3

## RESULTS

In this chapter, the results obtained using the mechanical fish will be discussed. The mechanical fish was used in this study to investigate the influence of different parameters which govern the forward propulsion of the fish.

Experiments were conducted for the C-start motion of the fish involving both the preparatory and propulsive strokes. The tests were conducted on a fish with a spine of thickness 0.4 mm and tails of trapezoidal shape with varying surface areas and stiffness.

A sample acceleration plot is shown in Figure 15 which compares the performance of the mechanical pike to that of live fish. A stainless steel tail with a surface area of 40.6 $cm^2$ was used (Tail 2). The body was bent from the straight line to 72° in 0.43 s and then was forcibly unbent. The duration of the overall process was 0.95 s.

The plot shows the forward acceleration of the fish. Velocity and displacement were obtained by performing numerical integration on the acceleration signal. The form of the acceleration, velocity and the displacement plots are similar to that observed by Harper and Blake in live fish and also later in a mechanical fish by Conte et al (2010).

It can be observed that there are two peaks in the acceleration plot. During stage 1, the fish had a negative acceleration as it moved backward. Stage 1 is followed by a delay period, shown by the red dotted lines, which varied depending on the angle of bending. During this period, the fish was not forced to bend or unbend. Stage 2 then began which corresponded to the propulsive stroke. The position of the mechanical fish through the bending and unbending is shown schematically in the acceleration plot.

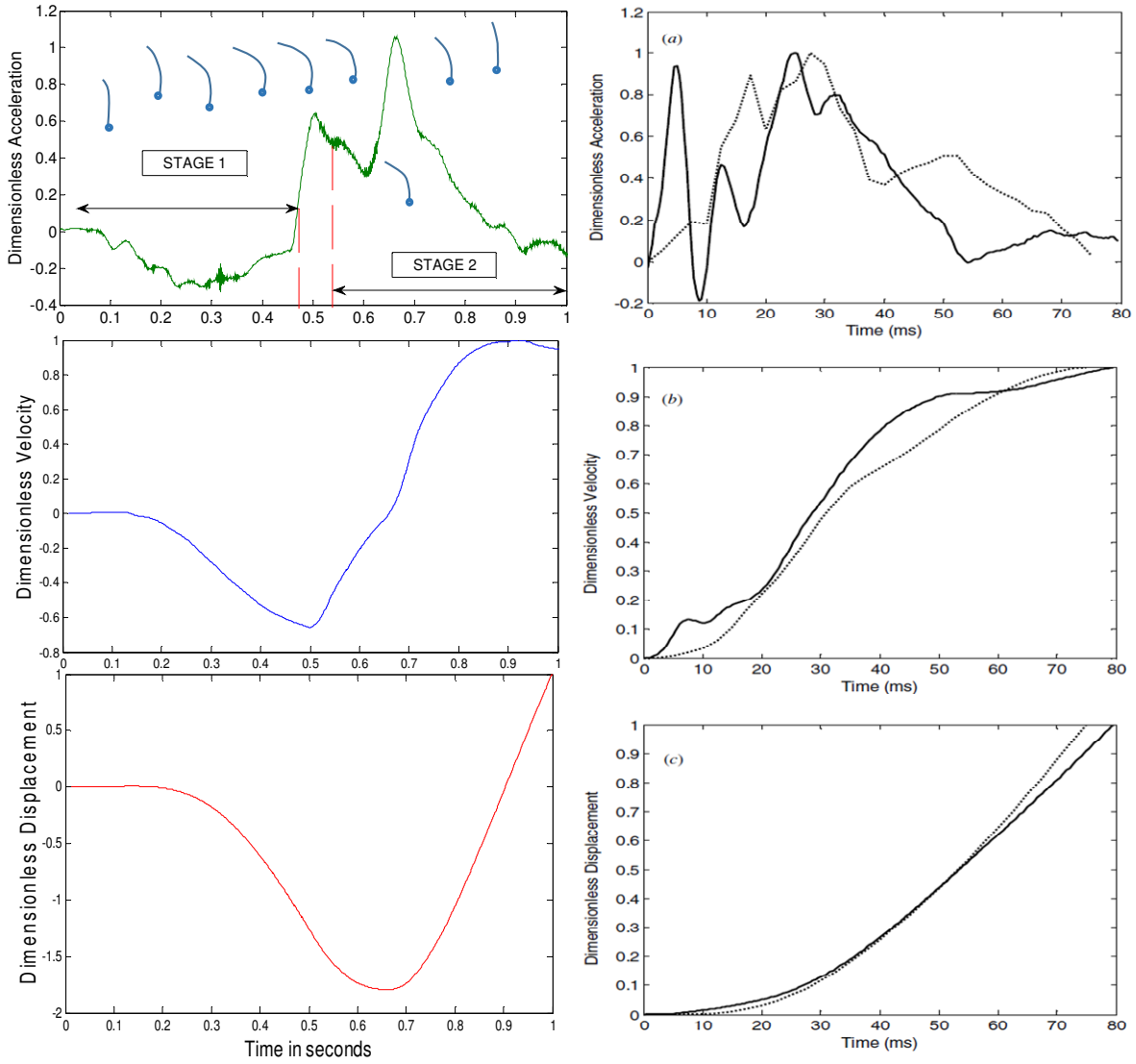


**Figure 15 (a) Sample Plot of Dimensionless Acceleration, Velocity and Displacement. 15 (b) Sample Acceleration, Velocity and Displacement of previous mechanical fish (continuous lines) and those of live fish (dotted lines) from Harper and Flake, Figure from Conte et. al. (2010).**

The two peaks were due to the two tail flips constituting stages 1 and 2. The first peak was generated by the tail flip due to the bending of the fish while the second peak was generated by the second tail flip caused by the unbending. The second tail beat involved the aggressive uncoiling of the fish. The fish body did not come to rest to a straight line position

immediately but continued to bend slightly in the opposite direction before finally coming to rest back to a straight line.

The acceleration, velocity and displacement curves shown in Figure 15 (a) were made dimensionless to compare it with the acceleration, velocity and displacement curves of the previous mechanical fish and that of the live fish.

All the recorded acceleration values were divided by the highest recorded acceleration to make it dimensionless. The same method was employed for making the velocity and displacement curves dimensionless.

**3.1.1 Tail 1:**

A trapezoidal shaped tail with a surface area of 40.6 $cm^2$ made of plastic was attached to the fish to see the influence of the tail on the acceleration of the fish. A sample acceleration plot is shown in Figure 16. The fish was bent starting from a straight line position at rest to an angle of 89° in 0.56 s and then forcibly unbent back to the straight line position. The duration of the propulsive stroke was 0.59 s. The entire process was 1.18 s in duration. A peak acceleration of 0.90 $m/s^2$ was recorded. The two peaks in the acceleration plot existed in this case as well; however, their magnitude was almost the same. The plastic tail had relatively low stiffness, which caused the tail to bend on its own apart from the rest of the fish body at small angles. This in turn increased the duration of the preparatory stroke.

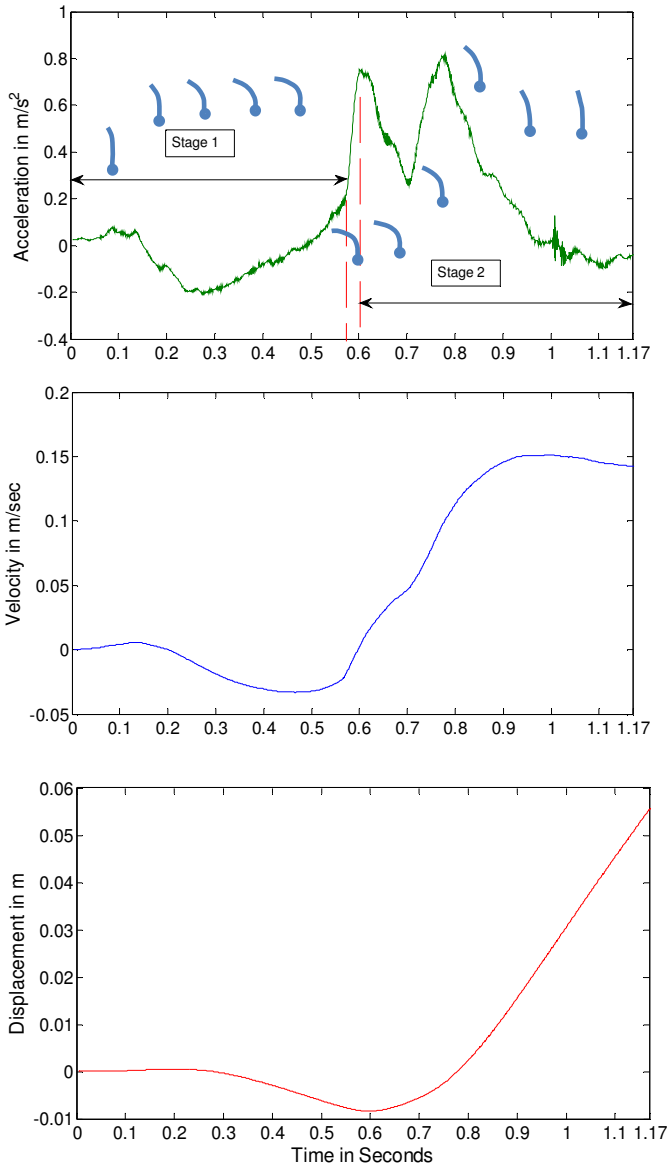


**Figure 16. Plot of Acceleration, Velocity and Displacement for Tail 1**

### 3.1.2 Tail 3

A series of tests were conducted on the fish with a trapezoidal shaped stainless steel tail with a surface area of 62.5 $cm^2$. The stiffness of tail 3 was the same as tail 2, but the surface area of the tail is increased for the case of the fish attached with tail 3 to investigate the influence of the surface area of the caudal fin on the acceleration of the fish. A sample plot showing the acceleration, velocity and displacement of the fish is shown in Figure 17.

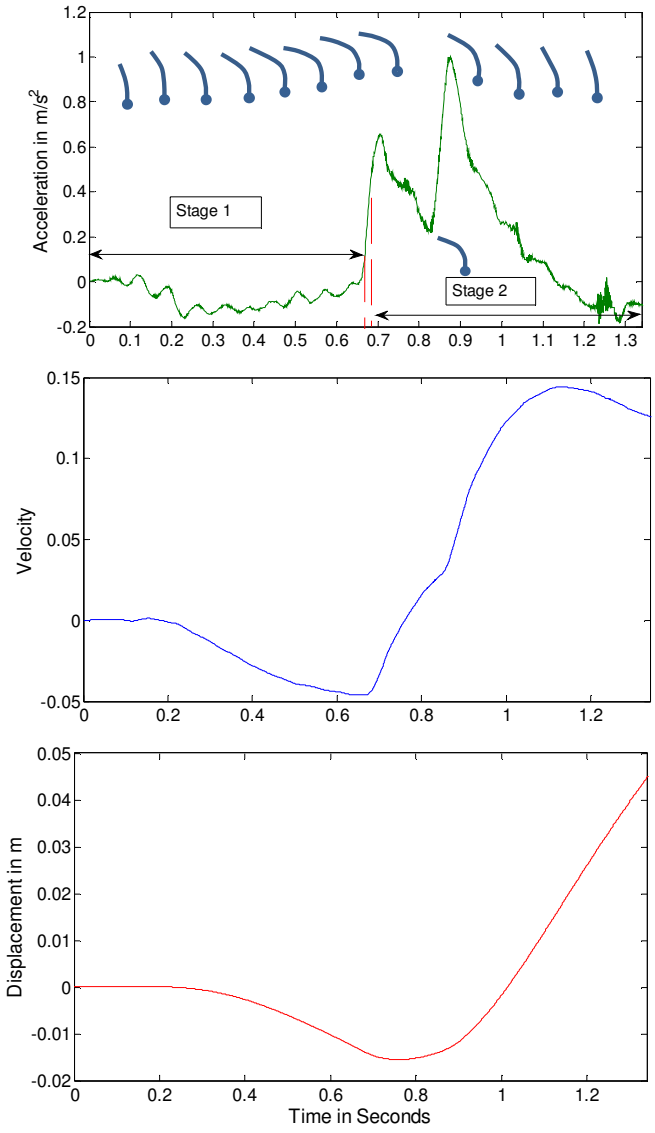


**Figure 17. Sample plot of Acceleration velocity and displacement for Tail 3**

The fish was bent to an angle of 76.2° in 0.66 s and forcibly unbent back to a straight line position in 0.65 s with a time delay of 0.023 s between the first and second stages. The entire process took 1.34 s to complete.

The maximum acceleration in the case shown in the figure was 1.1 m/s², which is slightly lower than the peak acceleration shown in Figure 15(a) and larger than the maximum

acceleration shown in Figure 16. The maximum velocity was 0.14 m/s which is slightly less than the velocity shown in Figure 16 and slightly more than the velocity shown in Figure 15

The total forward displacement was 10 cm, which was larger than that shown in Figure 16, which was 6 cm, and larger than that shown in Figure 15, which was 6 cm.

### 3.2 Time given for Stage 1

The time given for the preparatory stroke was the amount of time given to the servo motors to reach their designated target position. The servos tried to reach their target at the

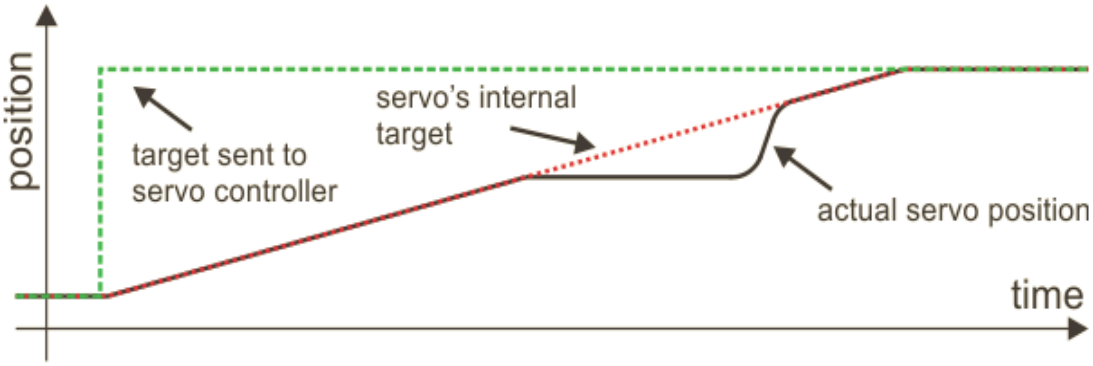


**Figure 18. Speed Control in Servo motors. (Figure from pololu.com)**

specified speed but it depended on the load on the servo whether it was able to reach the final position on time. An illustration of this is shown in Figure 18 where the servo takes a longer time to reach its desired position.

Since the closed loop between the servo and the microcontroller is not accessible, the actual time it took for the servo to reach its target could not be known. Instead the input to the servo, which was the time given to complete the task was known. The green dotted line in Figure 18 is the input signal to the servo. The red line is the actual target of the servo which cannot be readily known. The time given to the servo to reach its target at a fixed speed of rotation was directly related to the angle of bending of the fish.

The bending angle of the fish was calculated by capturing the motion of the fish using a high speed video camera at 240 fps, for different bending angles. These videos were then post-processed in a video analysis tool, Tracker, where the angle of bending of the fish was determined. Figure 19 shows the fish bent to a C-shape after the end of stage 1.

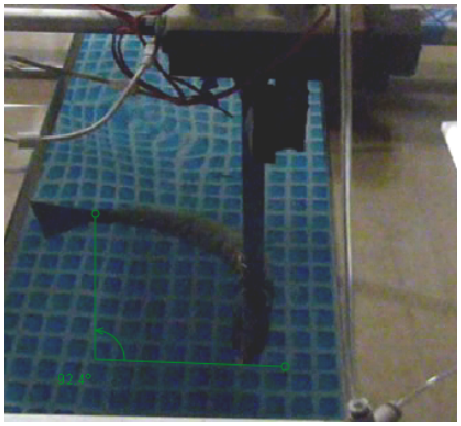

**Figure 19. Calculation of the bending curvature of the fish**

Two perpendicular lines were drawn from the head and tail of the fish and the angle formed by the two lines determined the bending curvature of the fish. Figure 20 shows the angle of bending of the fish with varying stroke-timings. Stroke-timing here means the amount of time given for the servo to complete the stroke and not necessarily the amount of time it took for the completion of stage1 as the fish continued to bend at small angles due to inertia even after the influence of the servo was no longer imposed. The plot shows a comparison of different tails and their angles of bending given different stroke timings. Tail 3 needs the longest time to reach its maximum bending angle due to the increased drag forces because of the large surface area. Among the three tails, Tail 2 needs the least time to reach its maximum angle of bending. The maximum angle of bending is different for each tail-case due to the changing properties of the caudal fin. The case with no tail attached has the highest bending

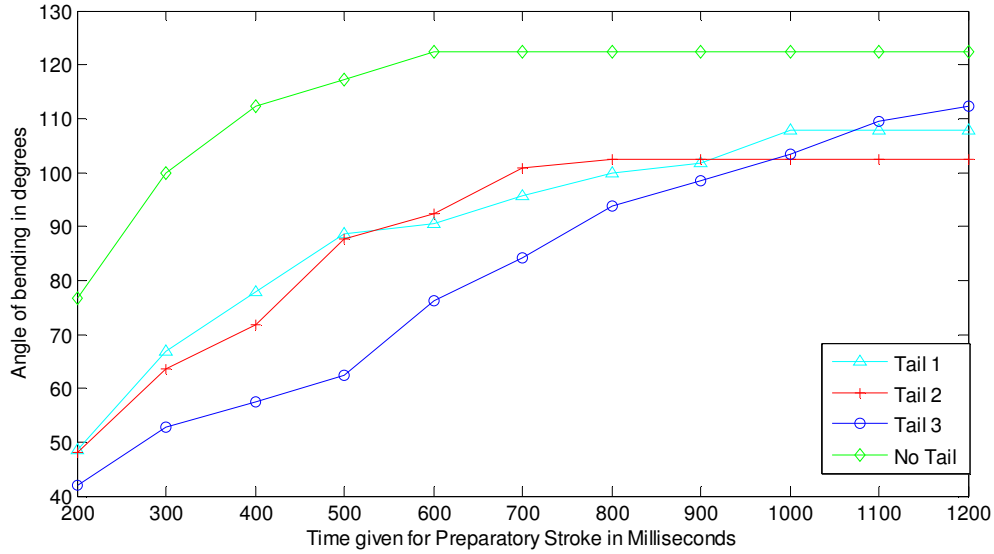


**Figure 20. Bending angle vs stroke timing**

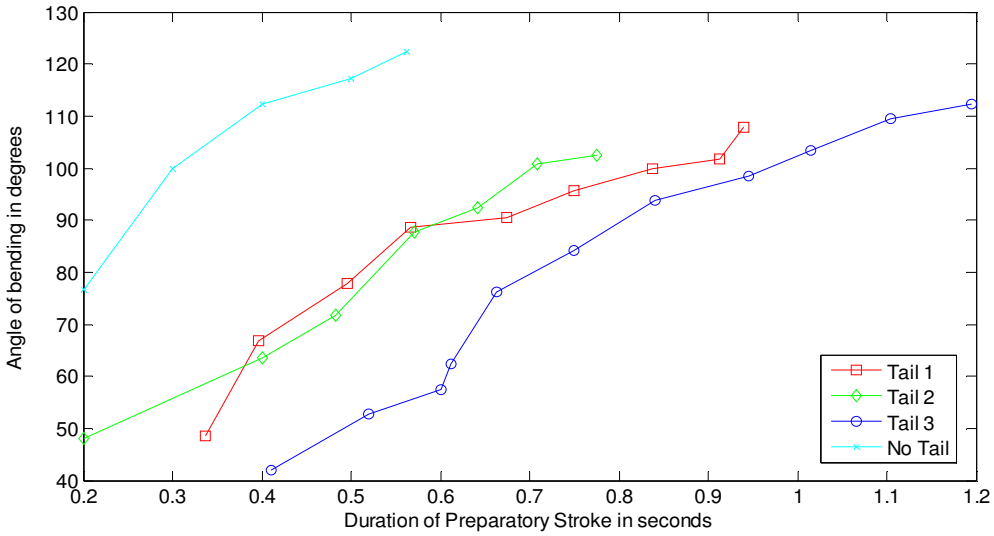


**Figure 21. Duration of Preparatory stroke vs bending angle**

angle and reaches its maximum angle of bending the fastest because it experiences the least drag force from the fluid.

Figure 21 shows the angle of bending of the fish for different tails and how it is dictated by the actual observed duration of Stage 1. The actual duration of stage 1 was calculated from the analysis of videos of the fish during the fast-start motion, at 240 frames per second. The angle of bending increased with the duration of stage 1 for all the tails since Stage 1 duration was directly dependent on the stroke-timing.

The propulsive stroke or Stage 2 of the fast-start motion of the fish largely contributes to the forward thrust achieved by the fish. The faster fish unbends, the more momentum it imparts to the fluid to achieve high accelerations. The duration of the propulsive stroke has to be minimum to ensure a high acceleration. But at the same time, the angle of bending of the fish should be sufficient to transfer the momentum from the uncoiling of the fish to the surrounding fluid. Figure 22 shows how the duration of the propulsive stroke changed with the

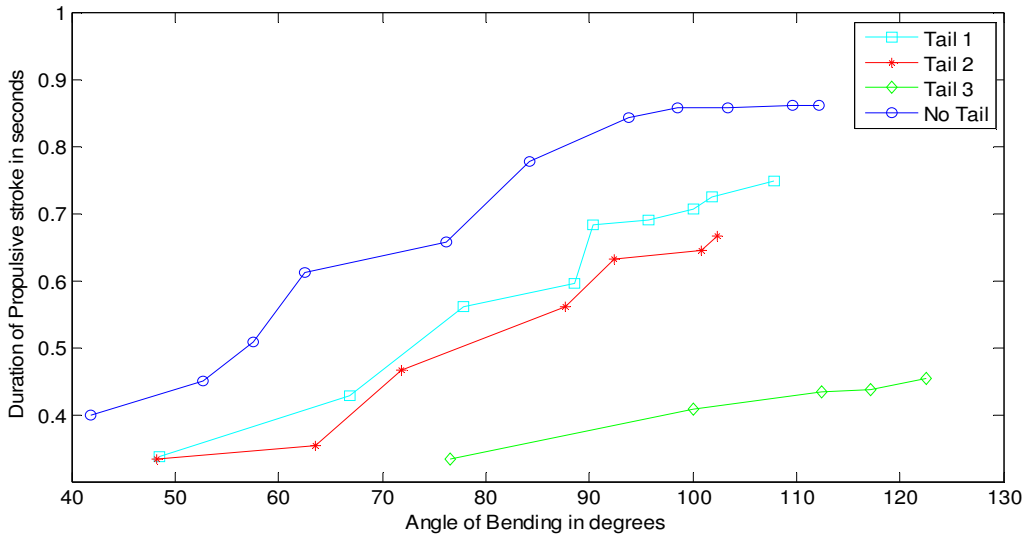


**Figure 22. Plot showing the change of Stage 2 duration with the bending angle of the fish**

angle of bending of the fish for different tails.

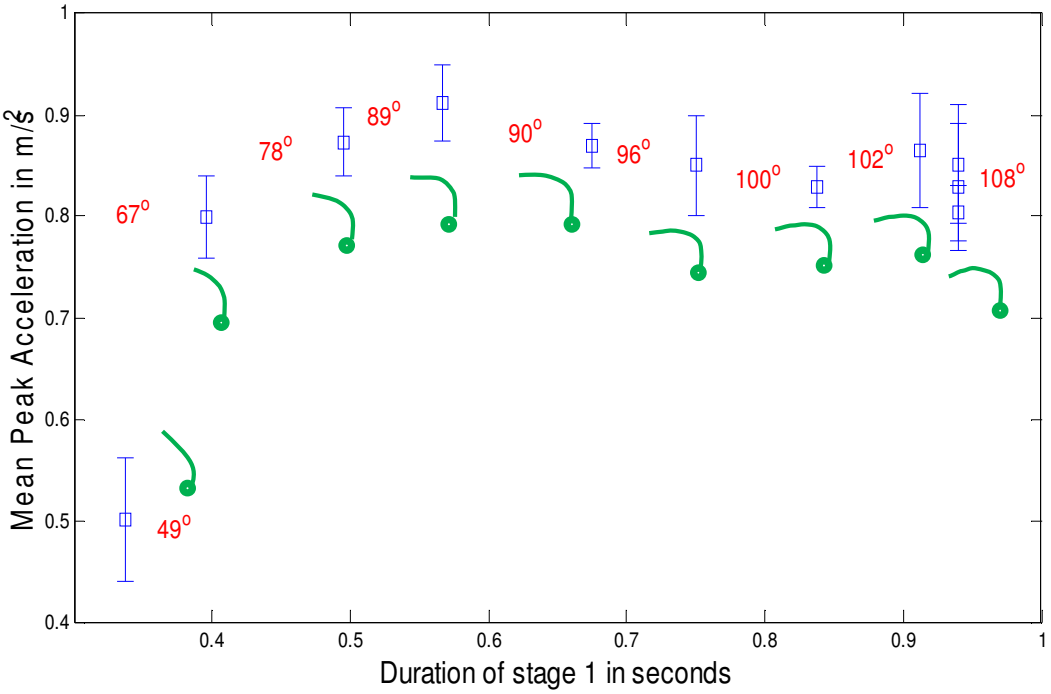


**Figure 23. Peak Acceleration vs. Stage 1 duration for Tail 1**

We can see that the duration of the propulsive stroke was minimum for Tail 2, as shown in Figure 22, at its maximum angle of bending compared to the other two tails. It would be useful to investigate the relationship between the type of tail being used, the bending angle and the duration of stages 1 and 2 to get a better understanding of the factors influencing the acceleration of the fish.

A series of tests were conducted for the fish with both the preparatory and propulsive stages. Three types of tails were tested. The spine used was a Spring Steel frame of 0.4 mm thickness. Ten trials each were conducted for different stroke timings which dictate the bending angle, duration of Stage 1 and Stage 2 and the time delay between the end of Stage 1 and the start of Stage 2.

The mean peak acceleration for each stroke timing over 10 trials is plotted with its standard deviation for the three tails. The results for Tail 1 are shown in Figure 23.

From the plot we can see that the mean peak acceleration increases with the duration of stage 1. The maximum acceleration was observed for a bending angle of 89$^{o}$ and almost remained almost constant for higher angles of bending until the duration of stage 1 is 0.9 s long. After this point there was a decrease in the mean peak acceleration even though the fish bent to the same angle.

Figure 24 shows the mean peak forward acceleration with varying angles of bending and Stage 1 duration for Tail 2. It is seen that the acceleration increased steadily for bending angles increasing in the range of 50$^{o}$ to 70$^{o}$ and for Stage 1 durations less than 0.5 s. Higher bending angles and Stage 1 durations exceeding 0.5 seconds resulted in a decrease in the mean peak

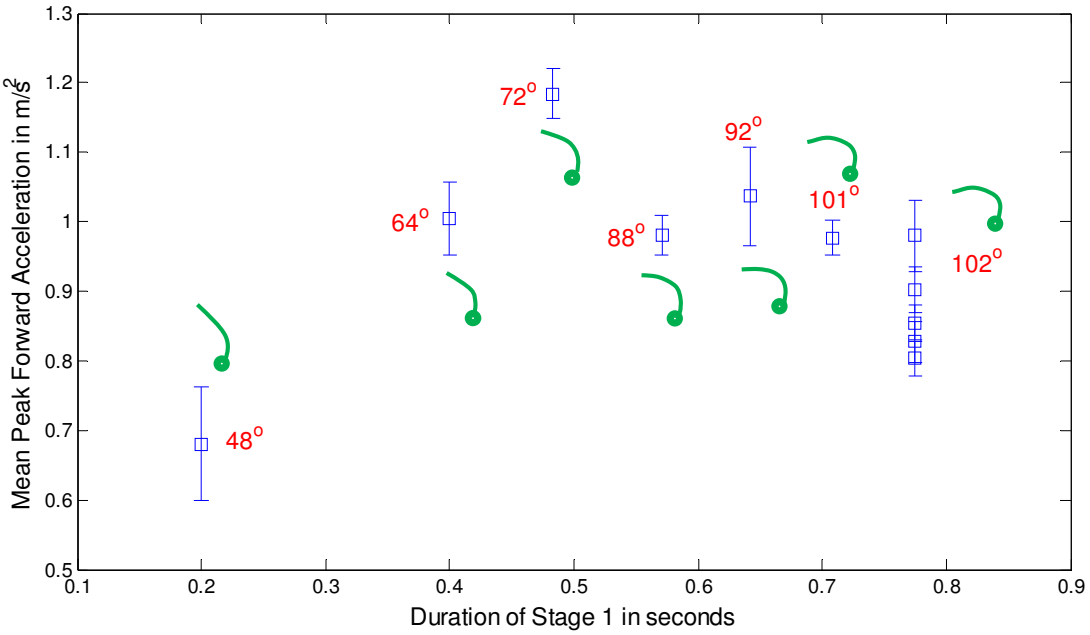


**Figure 24. Comparison of mean peak acceleration with Stage 1 duration for Tail 2**

acceleration. Then the peak acceleration dropped steadily when it reached its maximum bending angle and the delay between Stage1 and Stage 2 starts to become prominent.

Figure 25 shows the comparison of mean peak acceleration with varying Stage 1 duration and angle of bending for Tail 3. A similar trend of the acceleration was observed which

increased steadily till a particular angle of bending and Stage 1 duration and then decreased slightly and stayed the same for subsequent increase in bending angle and Stage 1 duration till it

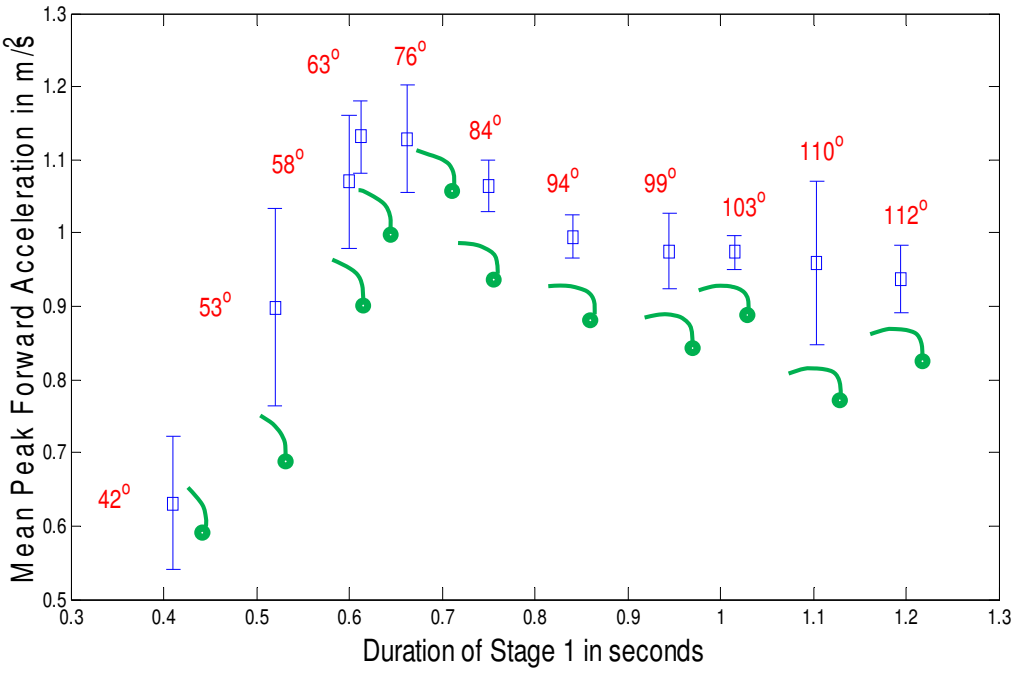


**Figure 25. Comparison with mean peak acceleration with Stage 1 duration for Tail 3**

reached its maximum angle of bending. There is no drop of acceleration after reaching the maximum angle of bending for Tail 3 compared to the other two tails because the delay between Stage1 and Stage 2 is not significant at that point. A significant delay here means any time delay greater than 0.1 s, which results in a decrease of peak acceleration as shown in Figure 26 and Figure 27.

### 3.3 Time delay between Stage1 and Stage 2

The time delay between the end of Stage 1 and the start of Stage 2 has an effect on the acceleration of the fish. Ahlborn (1997) proposed a reversal of momentum model which argues that the fast-start propulsion mechanism of the fish is achieved by using two counter-rotating vortices shed by the first and second tail-beat and the maximum acceleration is achieved when

the influence of the first vortex shed from Stage 1 is best utilized by the shed vortex from the propulsive stroke. If the time delay between the first and second stage increases, the strength of the first vortex decreases and eventually dissipates.

Tests were conducted to investigate the influence of the delay between Stage 1 and Stage 2 on the resulting peak acceleration. In each test, 10 trials were conducted for each

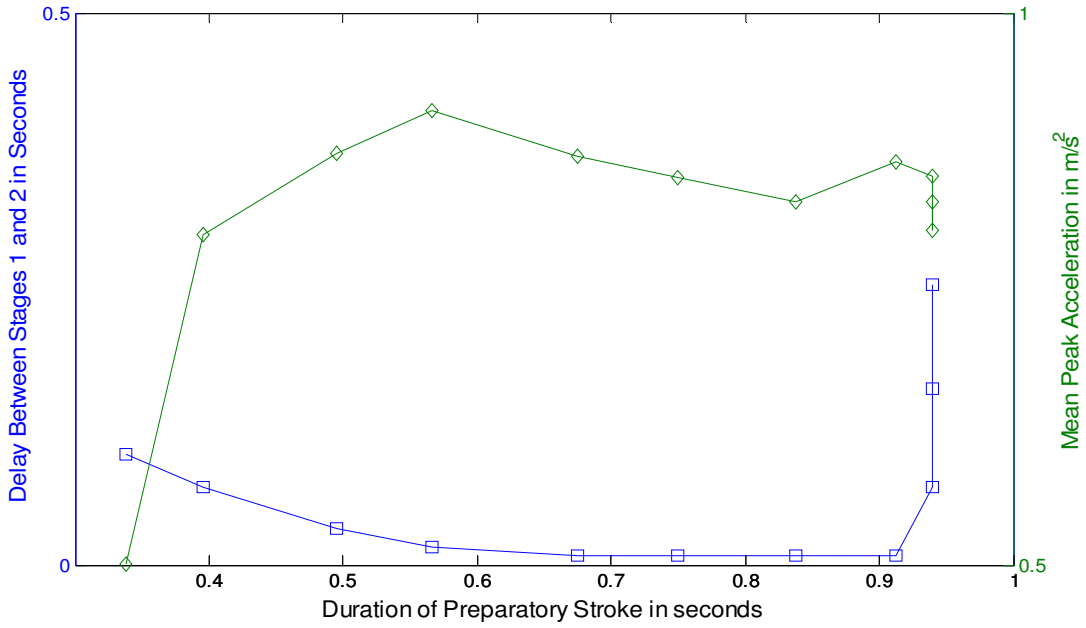


**Figure 26. Time delay and mean peak acceleration versus Stage 1 duration for Tail 1**

stroke-timing, which corresponded to a specific bending angle, duration of Stage 1, Stage 2, and the time delay between Stage 1 and Stage 2. The mean of the peak accelerations across 10 trials for each case was calculated and plotted against its corresponding Stage 1 duration and time delay for the three different tails. Figure 26 shows the time delay and the mean peak acceleration for the case where the fish was attached with Tail 1.

It was observed that the mean peak acceleration increased as the time delay decreased at the start and almost remained the same for the period during which the duration of the preparatory stroke increased but the time delay stays constant. After the duration of Stage 1

stopped increasing, the time delay steadily increased which resulted in a steady drop in the mean acceleration recorded. This figure shows an apparent relation between time delay and acceleration.

Figure 27 shows the relationship between time delay and mean acceleration across varying Stage 1 duration for Tail 2

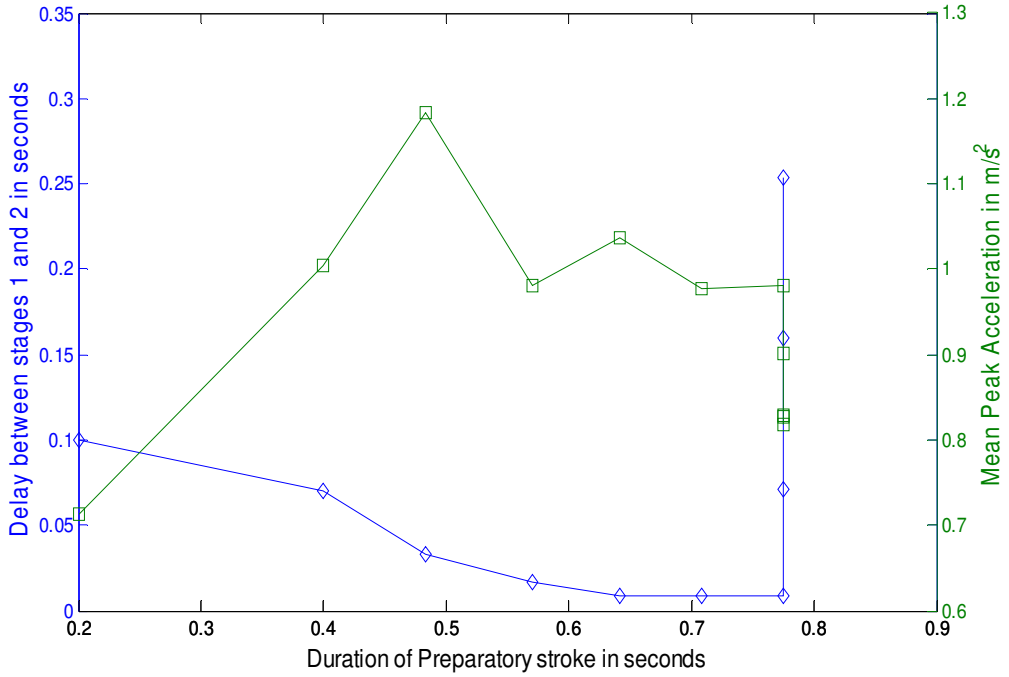


**Figure 27. Time delay and mean peak acceleration versus Stage 1 duration for Tail 2**

A pattern similar to the one observed in the case of Tail 1 is observed where the mean peak acceleration steadily increased when the time delay decreased, then decreased and stayed the same for a constant time delay. But the effect of the time delay was more prominent for tail 2 as there is a sharp drop in the mean acceleration along with a simultaneous steep increase in the time delay for a constant duration of Stage 1.

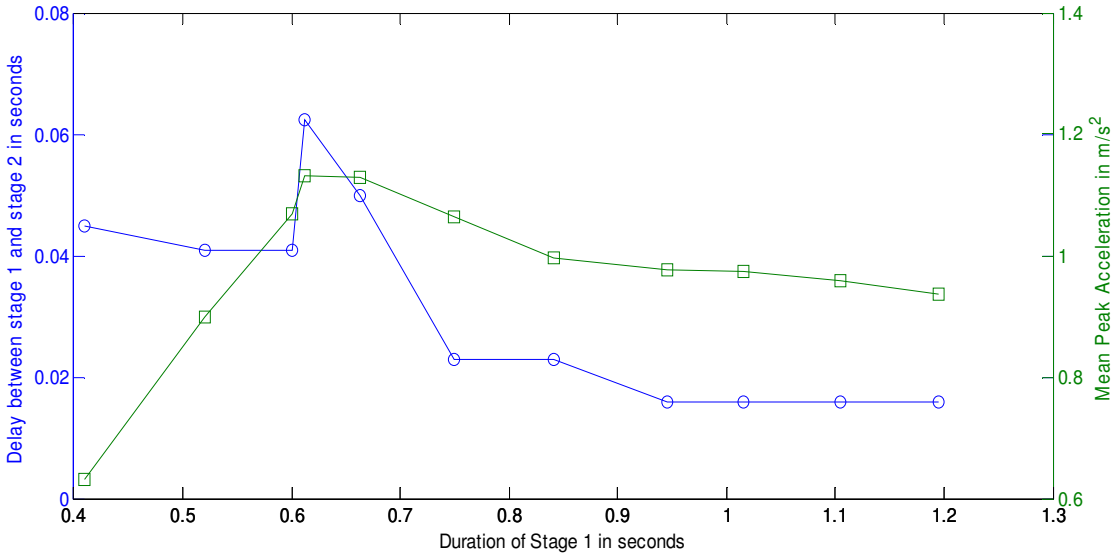


**Figure 28. Plot of Time Delay and mean peak acceleration over Stage 1 duration for Tail 3**

Figure 28 shows the plot of the mean peak acceleration and the time delay versus the Stage 1 duration for the case where the fish was attached with Tail 3. The series of tests conducted were similar to the ones conducted for the first two tails. Here again a steady increase in acceleration was observed for a corresponding decrease in time delay and a constant acceleration for a constant time delay. The only difference compared with the other two tails was that the Tail 3 case did not have a steady increase in time delay as it had a gradual increase in bending angle with the duration of Stage 1.

### 3.4 Tail Comparison

The acceleration of the fish with no tail attached was also investigated. The sample acceleration plot for such a case is shown in Figure 29. The form of the acceleration plot for the fish with no tail attached was different from the case when there was a tail. The acceleration

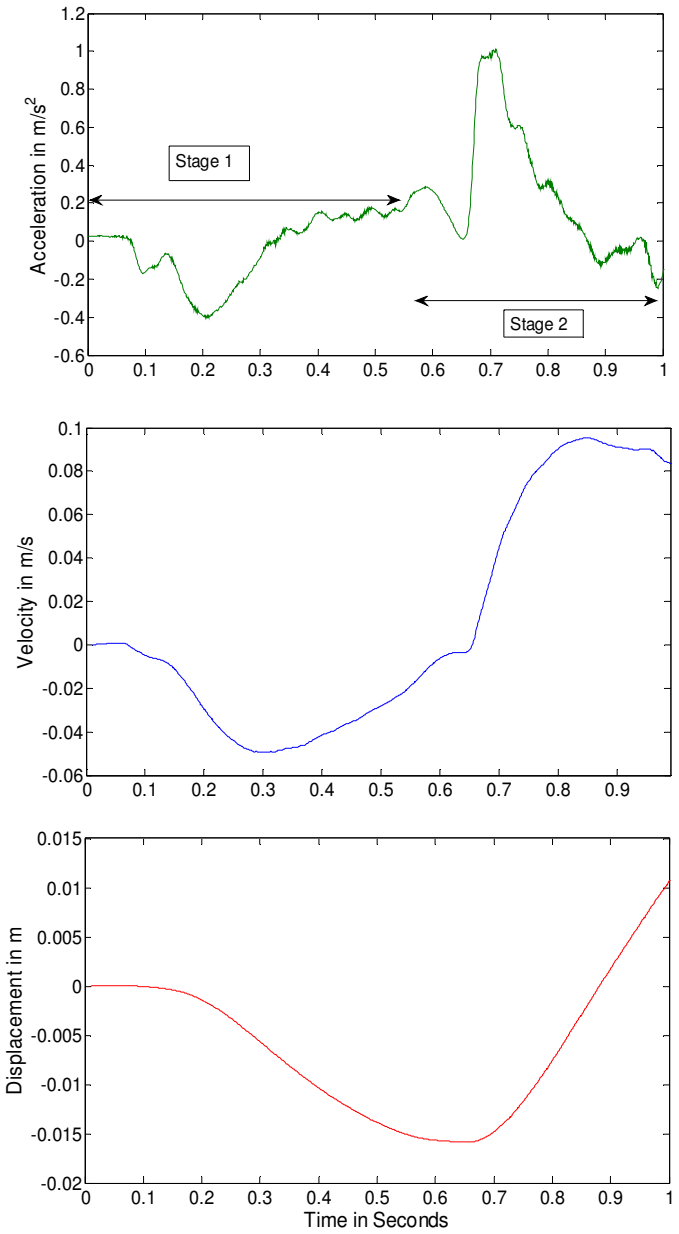


**Figure 29. Sample plot of Acceleration, Velocity and Displacement for No-tail**

plot had only one prominent peak as opposed to the two peaks seen in the cases with a tail.

From Figure 20, it is observed that all the different tail-types have approximately a common angle of bending at a certain point in the plot of bending angles, although the time taken to bend to that angle differs. Keeping the bending angle the same for all cases, an effective comparison can be made.

Figure 30 shows the effect of different tail types on the acceleration of the fish for

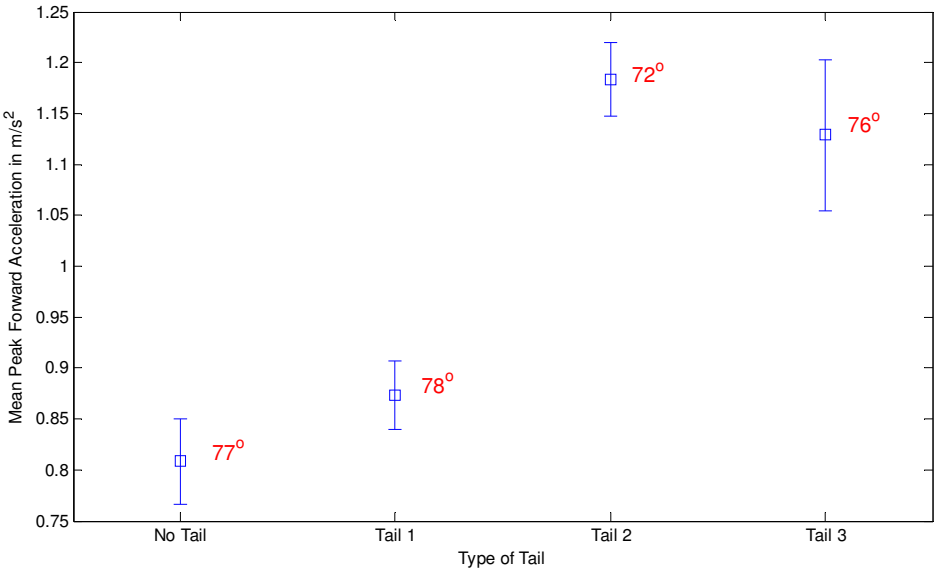


**Figure 30. Mean Peak Acceleration for different tails with approximately the same bending angle**

approximately the same bending angle. Tail 2 recorded the highest mean peak acceleration among the other cases. Tail 1 had low acceleration compared to the metal tails which suggests that tail stiffness did influence the acceleration of the fish. The size of the tail did not have a major influence on the forward acceleration as Tail 3 also recorded similar acceleration compared to Tail 2 with a smaller surface area.

### 3.4.1 The speed of Stage 1

The influence of the speed of bending to an angle during Stage 1 on the peak acceleration was investigated. A series of tests were conducted by bending the fish to an angle of 76$^{o}$ with varying speeds. An angle of 76$^{o}$ was chosen due to the fact that in Figure 25 this angle corresponded to the maximum recorded acceleration for Tail 3. Also, the maximum recorded acceleration for Tail 2 was at an angle of 72$^{o}$ as shown in Figure 24 which is close to 76$^{o}$. The speed of the second stage was set to a constant value which was the maximum speed of unbending. Ten trials were conducted for every case of Tail 2 and Tail 3. A sample acceleration plot for Tail 2 is shown in Figure 31.

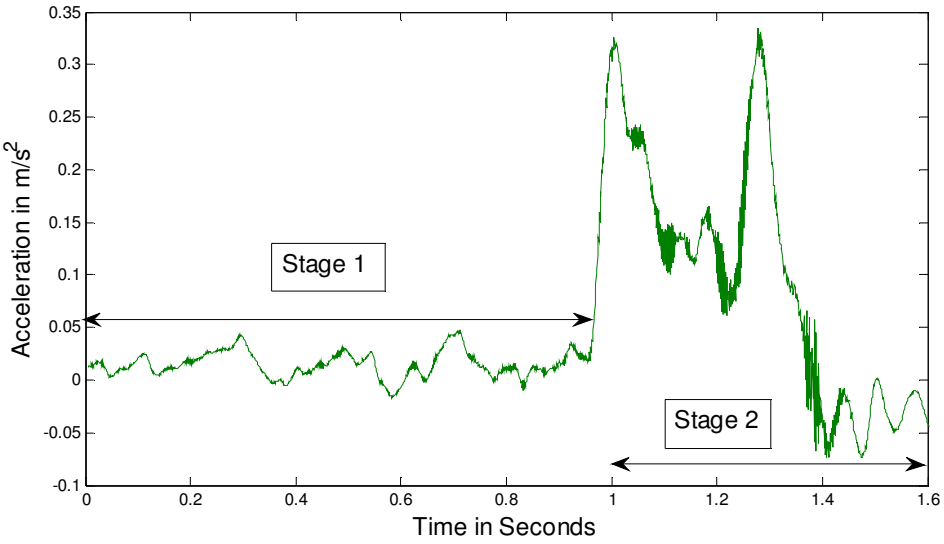


**Figure 31. Sample Acceleration plot for Tail 2 with reduced speed of bending for Stage 1**

As seen in this plot, the duration of stage 1 was much longer than the duration of stage 2. The fish was bent to an angle of 76$^{o}$ in 0.95 s and unbent to a straight line in 0.52 s. The first peak was generated when the fish was bent to its maximum angle. The peak acceleration recorded was about 0.5 m/s$^{2}$, which was lower than the peak observed in the case where the

fish was bent to approximately the same angle but at the maximum speed of bending as shown in Figure 15(a), resulting a peak acceleration of 1.2 $m/s^2$. The first peak in Figure 29 was about 0.35 $m/s^2$ compared to 0.8 $m/s^2$ in Figure 15(a). This showed that the speed of bending during stage 1 influenced the first peak in the acceleration plot, which in turn affected the second peak observed in the acceleration plots for the two cases.

The comparison of mean peak acceleration for varying speeds of stage 1 bending is shown in Figure 32. The peak acceleration decreased steadily as the speed of bending of Stage 1 decreased which resulted in a corresponding increase of the duration of Stage 1. The angle of bending at the end of Stage 1 and the speed of Stage 2 were unchanged across the three different speeds of Stage 1 bending.

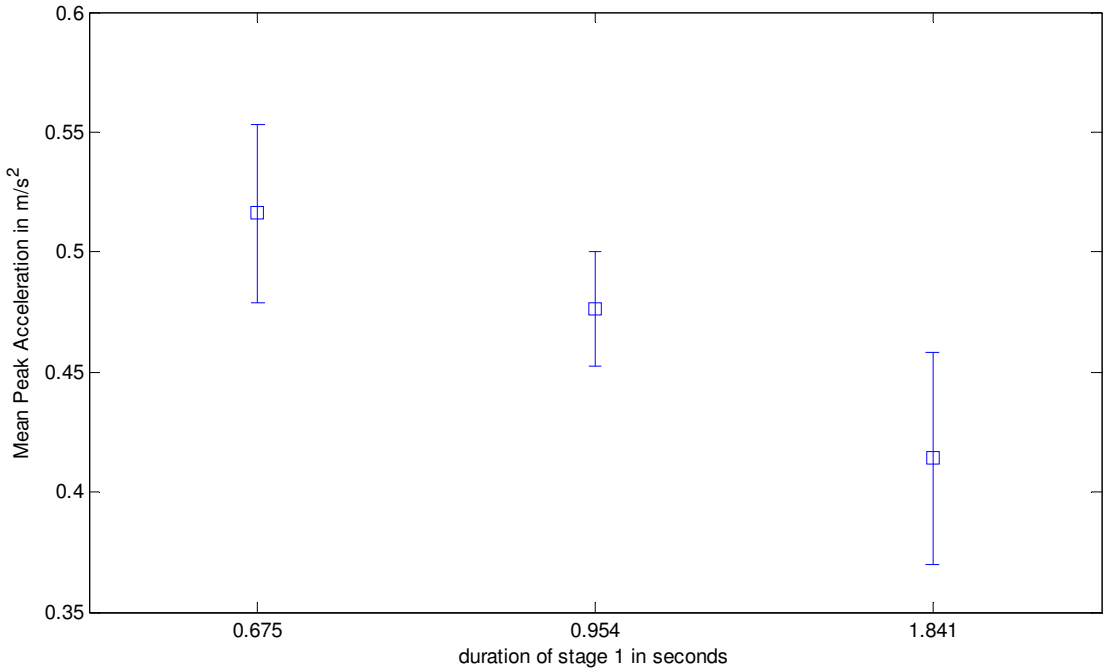


**Figure 32. Comparison of mean peak acceleration plot for Tail 2 for reduced speed of bending of Stage 1**

Similar tests were performed for the case with the fish attached with tail 3. A sample acceleration plot is shown in Figure 33. The fish was bent to an angle of 76$^o$ and then forcibly unbent back to a straight line position. The duration of Stage 1 was 0.975 s and the duration of Stage 2 was 0.55 s. A peak acceleration of about 0.8 m/s$^2$ was recorded which was smaller than the peak of 1.1 m/s$^2$ observed in Figure 17, corresponding to the acceleration for Tail 3 with the maximum speed of bending for stage 1. Here again it was observed that the duration of Stage 1 was longer than Stage 2 and the first peak recorded was lower than the first peak recorded in the plot shown in Figure 17. The first peak observed in this case was about 0.35 m/s$^2$ compared to the plot shown in Figure 17 which had a first peak of about 0.8 m/s$^2$.

Based on these plots it can be concluded that the speed of bending in Stage 1 influenced the peak acceleration. Ten trials were conducted for each case and the mean peak acceleration with the standard deviation is plotted in Figure 34

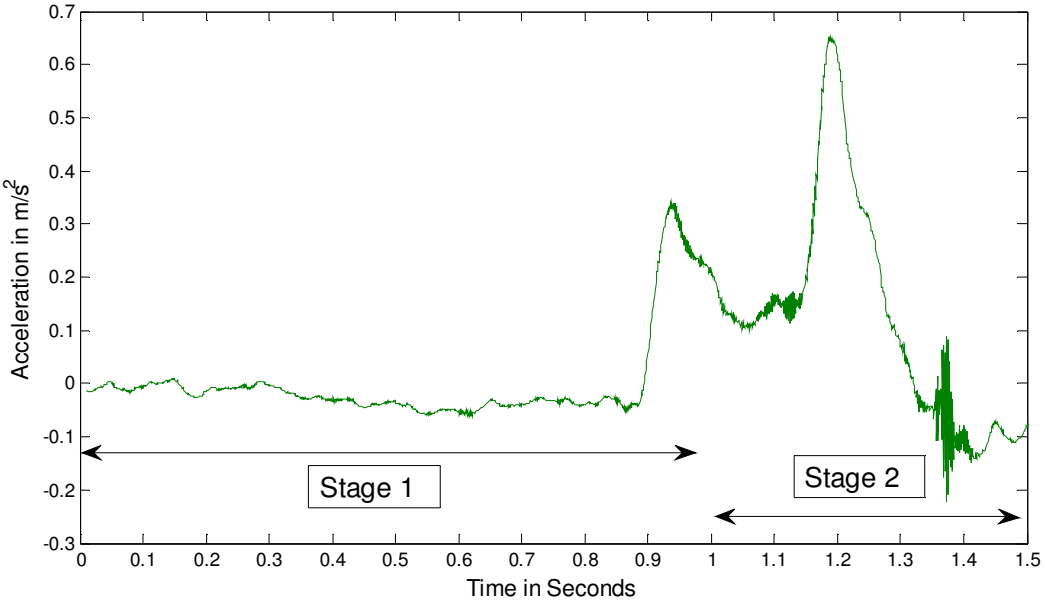


**Figure 33. Sample acceleration plot with reduced speed of bending of Stage 1 for Tail 3**

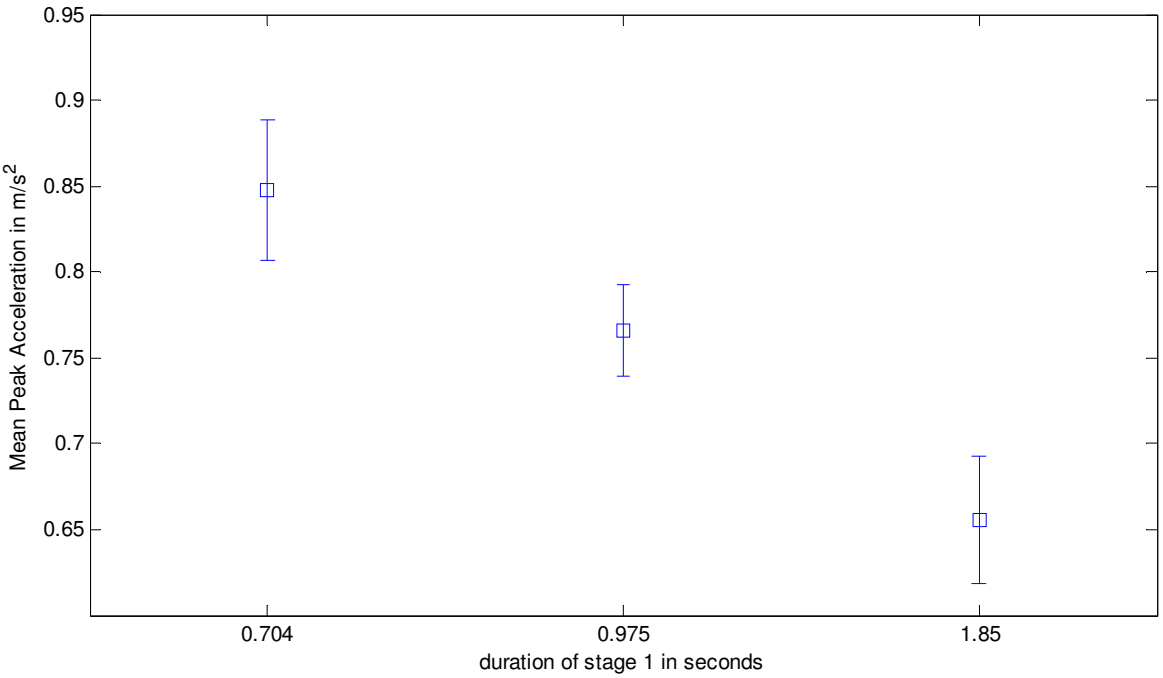


**Figure 34. Comparison of mean peak acceleration plot for Tail 3 for reduced speed of bending of Stage 1**

A steady decrease in the mean peak acceleration was observed with decreasing the speed of bending during Stage 1, which in turn corresponded to an increase in duration of Stage 1. The trend observed is similar to that of Tail 2 but the magnitude of the mean peak accelerations recorded were higher for Tail 3 compared to Tail 2.

# CHAPTER 4

# CONCLUSIONS

To understand the C-start of a mechanical fish, several factors were investigated in this study. The mechanical fish comprised of a PVC head attached to a spring steel frame, which acted as the spine of the fish. Aluminum ribs were attached to the spine such that the mechanical fish was morphologically similar to the live fish. High-torque servo motors were used as actuators which pulled on wire ropes threaded along the body of the fish, to bend and unbend the fish. The fish tail was attached to the caudal peduncle with the help of set-screws. The fish was suspended by a steel rod in a test section 96” x 59” x 24”. The rod was attached to a platform housing the servos, a microcontroller and an accelerometer. The platform was allowed to move in two dimensions by rods connected to the platform, which had end blocks mounted on air-bearings to facilitate frictionless motion.

A series of tests were performed to investigate the factors which influence the peak acceleration of the mechanical fish. A spring steel frame of 0.4 mm thickness was used for all the tests. Different types of tails with varying stiffness and surface areas were used to study the influence of the changing properties of the caudal fin on the forward acceleration of the fish.

The tests involved bending the fish to a certain angle by means of a servo and then forcibly unbending the fish back to a straight line position. The acceleration of the fish during these experiments was recorded using a 3-axis accelerometer with a sampling frequency of 1000 Hz, which was placed above the head of the fish and aligned with the axis of the fish. Several factors were investigated for their role in the acceleration of the fish. Tail stiffness, Tail surface area, angle of bending, duration of Stage 1 and Stage 2, time delay between Stage 1 and Stage 2 and the speed of bending of Stage 1 were among the parameters studied.

A typical acceleration plot for the mechanical fish attached with a tail, which was bent to a C-shape and then forcibly unbent back to a straight line had a negative acceleration at the start of the fish motion. This is followed by two peaks, which were qualitatively similar to that of the live fish and also to that of the previous mechanical fish. The two peaks observed were due to the two tail-beats corresponding to the bending of the fish to an angle starting from straight followed by the forcible unbending of the fish back to a straight line. The first peak was observed when the fish was bent to an angle at the end of Stage 1, which was followed by a delay. Then the second peak was observed when the fish was forcibly unbent back to a straight line. The magnitude of the first peak was less than that of the second peak suggesting that the majority of the thrust was generated by the propulsive stroke in Stage 2.

Tail 1 which was made of plastic and had a trapezoidal shape with a surface area of 40.6 $cm^2$, recorded the lowest accelerations compared to Tail 2 which was made of stainless steel and had a trapezoidal shape with a surface area of 40 $cm^2$ and Tail 3 which was made of the same material as Tail 2 but with a bigger surface area of 62 $cm^2$. The acceleration recorded by Tail 2 was slightly lower than that of Tail 3.

The duration of Stage 1 influenced the peak acceleration. The angle of bending increased with the duration of Stage 1 till the fish reached its maximum angle of bending. The mean peak acceleration for Tail 1 increased with the Stage 1 duration and bending angle. The highest peak acceleration of 0.9m/s² was recorded for a bending angle of 89°, which was less than the highest mean peak acceleration of 1.18 m/s² for Tail 2 and 1.13 m/s² for Tail 3.

The duration of Stage 2 increased with an increase in bending angle between 65° and 80°. A bending angle of about 75° recorded the highest peak accelerations for Tail 1, Tail 2 and Tail 3.

As the time delay between Stage 1 and Stage 2 increased after the fish had reached its maximum angle of bending, there was a corresponding decrease in the peak acceleration for Tails 1 and 2. Tail 3 did not have a steady decrease in peak acceleration as the time delay between Stage 1 and Stage 2 was almost the same because the fish gradually bent to its maximum angle of bending and there was not a long delay between Stage1 and Stage 2.

The duration of Stage 1 was much longer than Stage 2 and the first peak corresponding to the bending of the fish was smaller in magnitude compared to the case where the speed of Stage 1 was the maximum. The mean peak acceleration recorded decreased linearly with a corresponding decrease of the speed of Stage 1. Thus, it can be concluded that a tail with relatively high stiffness and a larger surface area with the minimum time delay between Stage 1 and Stage 2 required to take advantage of the vortices shed during Stage 1 before its influence diminishes, should be used to achieve high acceleration.

**BIBLIOGRAPHY**


Ahlborn, B., Chapman, S., Stafford, R., Blake, R. W., and Harper, D. G., "Experimental simulation of the thrust phases of fast start swimming of fish". *J. Exp. Biol.* **200** pp. 2301–2312, 1997

Barrett, D. S., Triantafyllou, M.S., Yue, D.K.P., Grosenbaugh, M.A. and Wolfgang, M.J., "Drag reduction in fish-like locomotion", *J. Fluid Mech*., vol. 392, pp. 183-212, 1999

Breder, C. M., "The locomotion of fishes," *Zoologica,* vol. 4, pp. 159–256, 1926.

Conte, J., Modarres-Sadeghi, Y., Watts, M.N., Hover, F.S., Triantafyllou, M.S., "A Fast-Starting Robotic Fish that Accelerates at 40 ms-2". *Journal of Bioinspiration and Biomimetics*, **5** 035004, 2010

Domenici, P.D. and Blake, R. W., "The kinematics and performance of fish fast-start swimming", *J. Exp. Biol*. **200**, 1165–78, 1997

Drucker, E.G. and Lauder, G.V., "Experimental Hydrodynamics of Fish Locomotion: Functional Insights from Wake Visualization", *Integr.and Comp. Biol.*,**42**, pp. 243-257, 2002

Eaton, R.C., Lavender, W.A., and Wieland C.M., "Identification of Mauthner-initiated response patterns in goldfish: Evidence from simultaneous cinematography and electro-physiology" *J. Comp. Physiol. A* **144**, pp. 521-531, 1981

Feng, C., Bonafilia, B., Modarres-Sadeghi, Y. and Triantafyllou, M.S., (2011), "The Mechanics of Fast-Start Performance of Pike Studied Using a Mechanical Fish" ASME 2011 International Mechanical Engineering Congress & Exposition, Denver, Colorado, November 14-16, 2011

Frith, H.R. and Blake, R.W., "The mechanical power output and hydromechanical efficiency of northern pike (Esox lucius) fast-starts", *J. Exp. Biol*. **198**, pp. 1863–73, 1995

Frith,H.R. and Blake, R.W., "Mechanics of the startle response in the northern pike, Esox Lucius", *Can. J. Zool*.**69** 2831–9, 1991.

Funch, P.G., Kinsman, S.L., Faber D.S., Koenig, E., and Zottoli, S.J., "Mauthner axon diameter and impulse conduction velocity decreases with growth of goldfish", *Neurosci. Lett*. **27**, pp.159-164, 1981

Gray, J., "Studies in animal locomotion. VI. The propulsive powers of the dolphin," *J. Exp. Biol*., vol. 13, pp. 192–199, 1936.

Harper D.G. and Blake R.W. "Prey capture and the fast-start performance of northern pike", Esox lucius *J. Exp. Biol*. **155** pp. 175–92, 1991.

Harper, D.G. and Blake, R.W., “Fast-start performance of rainbow trout *Salmo gairneri* and northern pike *Esox Lucius”, J. Exp. Biol.* **150,** pp. 321–42, 1990.

Lauder, G. V. and Tytell, E. D., *Fish Biomechanics*, Volume 23, pp. 444-445, 2006

Lauder, G. V. and Tytell, E. D., *Fish Biomechanics*, Volume 23, pp. 433-436, 2006

Lighthill, M.J. “Hydromechanics of aquatic animal propulsion: A survey.” *Ann. Rev. Fluid Mech*., **1**, pp. 413–446, 1969.

Lindsey, C. C., “Form, function and locomotory habits in fish,” in *Fish Physiology Vol. VII Locomotion*, W. S. Hoar and D. J. Randall, Eds. New York: Academic, 1978, pp. 1–100.

Michael Sfakiotakis, David M. Lane, and J. Bruce C. Davies, “Review of Fish Swimming Modes for Aquatic Locomotion”, *IEEE Journal of Oceanic Engineering*, Vol. 24, NO. 2, APRIL 1999

Triantafyllou, M. and G. S. Triantafyllou, “An efficient swimming machine”, *Sci. Amer*. **272**, pp. 64–70, 1995.

Webb, P.W., “Fast-start resistance of trout”, *J. Exp. Biol*. **96**, pp. 93–106, 1982

Webb, P.W., “Form and function in fish swimming,” *Sci. Amer.,* vol. 251, pp. 58–68, 1984.

Webb, P.W., “Is the high cost of body caudal fin undulatory swimming due to increased friction drag or inertial recoil?” *J. Exp. Biol*., vol. 162, pp. 157–166, 1992

Weihs, D. “The mechanism of rapid starting of slender fish”, *Biorheology*, **10**, pp. 343–50, 1973

Zottoli, S.J, “Correlation of the startle reflex and Mauthner cell auditory responses in unrestrained goldfish”, *J.Exp.Biol*, **66**, pp. 243-254, 1977